Renormalization group approach for highly anisotropic two-dimensional fermion systems: Application to coupled Hubbard chains

S. Moukouri
Department of Physics and Michigan Center for Theoretical Physics, University of Michigan, 2477 Randall Laboratory, Ann Arbor, Michigan 48109, USA

(Received 10 March 2008; revised manuscript received 23 May 2008; published 19 June 2008)

I apply a two-step density-matrix renormalization group method to the anisotropic two-dimensional Hubbard model. As a prelude to this study, I compare the numerical results to the exact one for the tight-binding model. I find a ground-state energy which agrees with the exact value up to four digits for systems as large as 24 $\times 25$. I then apply the method to the interacting case. I find that for strong Hubbard interaction, the ground state is dominated by magnetic correlations. These correlations are robust even in the presence of strong frustration. Interchain pair tunneling is negligible in the singlet and triplet channels and is not enhanced by frustration. For weak Hubbard couplings, due to interchain interaction, interchain nonlocal singlet pair tunneling is enhanced and magnetic correlations are strongly reduced. This suggests a possible superconductive ground state. The pairing mechanism is reminiscent of the Kohn-Luttinger mechanism.

DOI: 10.1103/PhysRevB.77.235116 PACS number(s): 71.10.Fd, 75.40.Mg

I. INTRODUCTION

The intriguing discovery of superconductivity (SC) lying next to antiferromagnetism (AFM) in the phase diagram of the charge-transfer Bechgaard salts (see Fig. 1) remains one of the most intriguing issues of condensed-matter physics.[1–3] The proximity of AFM and SC turned out to be a generic feature not only of the Bechgaard salt series $(TMTSF)_2X$, but also of the Fabre salts $(TMTTF)_2X$ and layered two-dimensional (2D) organic and cuprate superconductors. In the quasi-one-dimensional (1D) organic materials, AFM occupies a large region of the experimental phase diagram (see Fig. 1) and is believed to be central to the emergence of SC. It is believed that the understanding of AFM is a prerequisite to that of SC.

The nature of pairing in these compounds is still unclear. Recent experiments have yielded conflicting results. A NMR Knight-shift experiment by Lee *et al.*[4] found that the symmetry of the Cooper pairs is triplet in $(TMTSF)_2(PF)_6$. No shift was found in the magnetic susceptibility at the transition for measurement made under a magnetic field of about 1.4 T. A subsequent Knight-shift experiment performed at lower fields reveals a decrease in the spin susceptibility.[5] This result is consistent with singlet pairing. Shinagawa *et al.*[5] suggested a possible singlet-triplet pairing crossover as a function of the magnetic field as a resolution of these conflicting results.

In the face of these experimental uncertainties, a theoretical input onto the behavior of simple models of these compounds is of crucial importance. A theoretical analysis of AFM in the quasi-1D organic materials was proposed by Bourbonnais and Caron.[6] This description was essentially based on a perturbative renormalization group (RG) applied on the g-ology model. They found that the AFM phase has two regions. On the left side of the AFM phase, the 1D chains are Mott insulators; the charge gap Δ_ρ induced by coulomb interactions is such that $\Delta_\rho \gg t_\perp$, where $t_\perp$ is the transverse hopping parameter. Hence, the single-particle transverse hopping is irrelevant. In this region, the electrons are necessarily confined in the chains. $t_\perp$ can nevertheless generate an interchain exchange $J_\perp$ by virtual interchain hopping. Using the RG method,[7] it can be shown that this process leads to a transverse effective Hamiltonian $H_\perp = \int dx \Sigma_i J_\perp S(x)_i S(x)_{i+1}$, with $J_\perp \approx t_\perp^2/\Delta_\rho$. In this region, the electrons are necessarily confined in the chains due to the irrelevance of $t_\perp$. As pressure increases, the electrons progressively delocalize in the transverse direction. In the right region of the AFM phase, the magnetism is itinerant and arises from the nesting of the Fermi surface $\epsilon_{r,l}(k) = -\epsilon_{l,r}(k+Q)$, where the indices (r,l) stand for the right and the left parts of the Fermi surface, respectively, and $Q=(2k_F,\pi)$ is the nesting momentum. The nesting leads to the divergence of the susceptibility $\chi(Q,\omega=0) \propto \frac{1}{L^2}\Sigma_k \frac{f[\epsilon_r(k)]-f[\epsilon_l(k+Q)]}{\epsilon_r(k)-\epsilon_l(k+Q)}$. Further increasing pressure destroys the magnetic order and leads to superconductivity as illustrated on the right part of the phase diagram of Fig. 1.

While magnetism is now quite well understood in the quasi-1D materials, the same cannot be said for superconductivity. The relation between magnetism and superconductivity remains unclear. In this paper, starting from a single chain, I analyze the effects of small transverse hoppings and

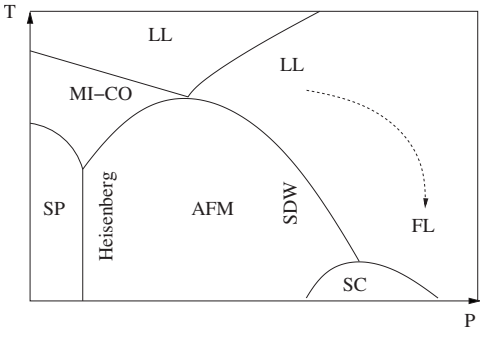

FIG. 1. Sketch of generic experimental phase diagram of the quasi-1D organic conductors: Luttinger liquid (LL), Fermi liquid (FL), Mott insulator (MI), charge ordering (CO), spin-Peierls (SP), antiferromagnet (AFM), and superconductor (SC).

interactions using the two-step density-matrix renormalization group (TSDMRG) method.[8,9] I find, in agreement with the work of Bourbonnais and Caron,[6,7] that magnetism is dominant in the strong and intermediate coupling regimes. There is a small region of parameters in the weak-coupling regime where magnetism is suppressed in favor of singlet superconductivity. The mechanism of pair hopping is reminiscent of the Kohn-Luttinger (KL) effect.[10]

II. MODEL

The essential features of the phase diagram of the organic conductors may be captured by the anisotropic Hubbard model (AHM) at quarter filling,

$$H = -t_{\parallel}\sum_{i,l,\sigma}(c^{\dagger}_{i,l,\sigma}c_{i+1,l,\sigma}+\text{H.c.}) + U\sum_{i,l} n_{i,l,\uparrow}n_{i,l,\downarrow} + V\sum_{i,l} n_{i,l}n_{i+1,l} - \mu\sum_{i,l,\sigma} n_{i,l,\sigma} - t_{\perp}\sum_{i,l,\sigma}(c^{\dagger}_{i,l,\sigma}c_{i,l+1,\sigma}+\text{H.c.}), \tag{1}$$

or a more general Hubbard-like model including longer range Coulomb interactions. The indices i and l label the sites and the chains, respectively. For these highly anisotropic materials, $t_{\perp} \ll t_{\parallel}$. Over the years, the AHM has remained a formidable challenge to condensed-matter theorists. Some important insights into this model or its low energy version, the g-ology model, have been obtained through the work of Giamarchi[3] and Bourbonnais and Caron.[6] They used a perturbative renormalization group approach to analyze the crossover from 1D to 2D at low temperatures. More recently, Biermann *et al.*[11] applied the chain dynamical mean-field approach to study the crossover from Luttinger liquid to Fermi liquid in this model. Despite this important progress, crucial information such as the ground-state phase diagram, or most notably, whether the AHM displays superconductivity, still haven't gained consensus. So far it has remained beyond the reach of numerical methods such as the exact diagonalization (ED) or the quantum Monte-Carlo (QMC) methods. ED cannot exceed lattices of about 4×5. It is likely to remain so for many years unless there is a breakthrough in quantum computations. The QMC method is plagued by the minus sign problem and will not be helpful at low temperatures. The small value of $t_{\perp}$ implies that, in order to see the 2D behavior, it will be necessary to reach lower temperatures than those usually studied for the isotropic 2D Hubbard model. Hence, even in the absence of the minus sign problem, in order to work in this low-temperature regime, the QMC algorithm requires special stabilization schemes which lead to prohibitive cpu time.[12]

III. TWO-STEP DMRG

I have shown in Ref. 8 that this class of anisotropic models may be studied using a TSDMRG method. The TSDMRG method is a perturbative approach in which the standard 1D DMRG is applied twice. In the first step, the usual 1D DMRG method[13] is applied to find a set of low lying eigenvalues ϵ_n and eigenfunctions $|\phi_n\rangle$ of a single chain. In the second step, the 2D Hamiltonian is then projected onto the basis constructed from the tensor product of the $|\phi_n\rangle$s. This projection yields an effective one-dimensional Hamiltonian for the 2D lattice

$$\tilde{H} \approx \sum_{[n]} E_{\|[n]}|\Phi_{\|[n]}\rangle\langle\Phi_{\|[n]}| - t_{\perp}\sum_{i,l,\sigma}(\tilde{c}^{\dagger}_{i,l,\sigma}\tilde{c}_{i,l+1,\sigma}+\text{H.c.}), \tag{2}$$

where $E_{\|[n]}$ is the sum of eigenvalues of the different chains, $E_{\|[n]}=\Sigma_l \epsilon_{n_l}$; $|\Phi_{\|[n]}\rangle$ are the corresponding eigenstates, $|\Phi_{\|[n]}\rangle = |\phi_{n_1}\rangle|\phi_{n_2}\rangle\ldots|\phi_{n_L}\rangle$; $\tilde{c}^{\dagger}_{i,l,\sigma}$, $\tilde{c}_{i,l,\sigma}$, and $\tilde{n}_{i,l,\sigma}$ are the renormalized matrix elements in the single chain basis. They are given by

$$(\tilde{c}^{\dagger}_{i,l,\sigma})^{n_l,m_l} = (-1)^{n_i}\langle\phi_{n_l}|c^{\dagger}_{i,l,\sigma}|\phi_{m_l}\rangle, \tag{3}$$

$$(\tilde{c}_{i,l,\sigma})^{n_l,m_l} = (-1)^{n_i}\langle\phi_{n_l}|c_{i,l,\sigma}|\phi_{m_l}\rangle, \tag{4}$$

$$(\tilde{n}_{i,l,\sigma})^{n_l,m_l} = \langle\phi_{n_l}|n_{i,l,\sigma}|\phi_{m_l}\rangle, \tag{5}$$

where n_i represents the total number of fermions from sites 1 to $i-1$. For each chain, operators for all the sites are stored in a single matrix

$$\tilde{c}^{\dagger}_{l,\sigma} = (\tilde{c}^{\dagger}_{1,l,\sigma},\ldots,\tilde{c}^{\dagger}_{L,l,\sigma}), \tag{6}$$

$$\tilde{c}_{l,\sigma} = (\tilde{c}_{1,l,\sigma},\ldots,\tilde{c}_{L,l,\sigma}), \tag{7}$$

$$\tilde{n}_{l,\sigma} = (\tilde{n}_{1,l,\sigma},\ldots,\tilde{n}_{L,l,\sigma}). \tag{8}$$

Since the in-chain degrees of freedom have been integrated out, the interchain couplings are between the block matrix operators in Eqs. (6) and (7) which depend only on the chain index l. In this matrix notation, the effective Hamiltonian is one-dimensional and it is also studied by the DMRG method. The only difference compared to a normal 1D situation is that the local operators are now $ms_2\times ms_2$ matrices, where ms_2 is the number of states kept during the second step.

The two-step method has previously been applied to anisotropic two-dimensional Heisenberg models.[8] In Ref. 9, it was applied to the $t-J$ model, but due to the absence of an exact result in certain limits, it was tested against ED results on small ladders only. A systematic analysis of its performance on a fermionic model on 2D lattices of various sizes has not been done. In this paper, as a prelude to the study of the AHM, I will apply the TSDMRG to the anisotropic tight-binding model on a 2D lattice, i.e., model (1) with $U=V=0$. I perform a comparison with the exact result of the tight-binding model. I was able to obtain agreement for the ground-state energies on the order of 10^{-4} for lattices of up to 24×25. I then discuss how these calculations may be extended to the interacting case, before presenting the $U\neq 0$ results.

Additional insight in the behavior of H may be gained by using the Wilson RG instead of DMRG in the second step. The advantage of the Wilson RG lies in the fact that the low energy spectrum can be obtained. However, the Wilson method directly applied to $\tilde{H}$ is not accurate, because all the terms in the transverse direction are of the same order. I use the same trick used by Wilson for the Kondo problem.[14] $\tilde{H}$ is

defined as the limit of $\tilde{H}_\Lambda$ when $\Lambda \to 1$. $\tilde{H}_\Lambda$ is given by

$$\tilde{H}_\Lambda = \sum_l \frac{H_{l,l+1}}{\Lambda^{(l-1)/2}}, \tag{9}$$

where

$$H_{l,l+1} = H_{0,l} + H_{0,l+1} - t_\perp \sum_\sigma (\tilde{c}^\dagger_{l,\sigma} \tilde{c}_{l+1,\sigma} + \text{H.c.}).$$

It is to be noted that this is not the usual Wilson's momentum space discretization. The justification of this scheme rests on the fact that the essential physics remains unchanged by the introduction of Λ. When $\Lambda > 1$, the terms corresponding to $l > 1$ act as a perturbation on the term with $l = 1$. For Λ not too large, I expect $\tilde{H}_\Lambda$ to essentially have the same behavior as $\tilde{H}$. But if $\Lambda \gg 1$, $t_\perp / \Lambda$ will be too small with respect to the finite-size energy separation and the chains will be disconnected. It is to be remarked that this approach may also be useful if it is embedded as a cluster solver in a chain-dynamical mean-field approach.[11]

IV. WARM UP: THE TIGHT-BINDING MODEL

The tight-binding Hamiltonian is diagonal in the momentum space; the single-particle energies are

$$\epsilon_k = -2t_\parallel \cos k_x - 2t_\perp \cos k_y - \mu, \tag{10}$$

where $k=(k_x,k_y)$, $k_x = n_x \pi/(L_x+1)$ and $k_y = n_y \pi/(L_y+1)$ for open boundary conditions (OBC); L_x, L_y are, respectively, the linear dimensions of the lattice in the parallel and transverse directions. The ground-state energy of an N electron system is obtained by filling the lowest states up to the Fermi level $E_{[0]}(N) = \Sigma_{k<k_F} \epsilon_k$. However, in real space, this problem is not trivial and it constitutes, for any real-space method such as the TSDMRG, a test having the same level of difficulty as the case with $U \neq 0$. This is because the term involving U is diagonal in real space and the challenge of diagonalizing the AHM arises from the hopping term.

I will study the tight-binding model at quarter filling $N/L_xL_y = 1/2$, the nominal density of the organic conductors known as the Bechgaard salts. Systems of up to $L_x \times L_y = L \times (L+1) = 24 \times 25$ will be studied. During the first step, I

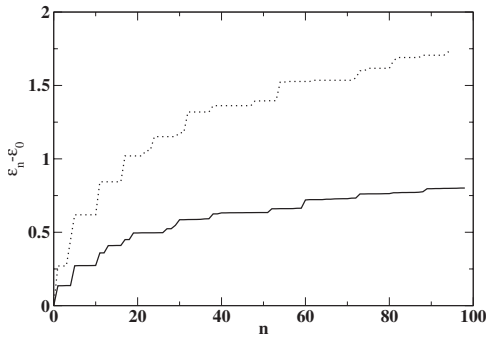

FIG. 2. Low-lying states of the 1D tight-binding model (full line) and of the 1D Heisenberg spin chain (dotted line) for $L=16$ and $ms_2=96$.

TABLE I. Transverse hopping and chemical potential used in the simulations for different lattice sizes

	8×9	16×17	24×25
$t_\perp$	0.28	0.15	0.1
μ	−1.2660	−1.3411	−1.3657
$\Delta\epsilon/t_\perp$	6.42	5.40	5.78

keep enough states (ms_1 is a few hundred) so that the truncation error ρ_1 is less than 10^{-6}. I target the lowest state in each charge-spin sectors $N_x \pm 2$, $N_x \pm 1$, N_x and $S_z \pm 1$, $S_z \pm 2$, N_x is the number of electrons within the chain. It is fixed such that $N_x/L_x = 1/2$. There are a total of 22 charge-spin states targeted at each iteration.

For the tight-binding model, the chains remain disconnected if $t_\perp < \epsilon_0(N_x+1) - \epsilon_0(N_x)$ or $t_\perp < \epsilon_0(N_x) - \epsilon_0(N_x-1)$, where N_x is the number of electrons on single chain. In order to observe transverse motion, it is necessary that at least $t_\perp \gtrsim \epsilon_0(N_x+1) - \epsilon_0(N_x)$ and $t_\perp \gtrsim \epsilon_0(N_x) - \epsilon_0(N_x-1)$. These two conditions are satisfied only if μ is appropriately chosen. The values listed in Table I corresponds to $\mu = [\epsilon_0(N_x+1) - \epsilon_0(N_x-1)]/2$. This threshold varies with L. I give in Table I the values of $t_\perp$ chosen for different lattice sizes. In principle, for the TSDMRG to be accurate, it is necessary that $\Delta\epsilon = \epsilon_{n_c} - \epsilon_0$, where ϵ_{n_c} is the cutoff, be such that $\Delta\epsilon/t_\perp \gg 1$. But in practice, I find that I can achieve accuracy up to the fourth digit even if $\Delta\epsilon/t_\perp \approx 5$ using the finite system method. Five sweeps were necessary to reach convergence. Note that this conclusion is somewhat different from my earlier estimate of $\Delta\epsilon/t_\perp \approx 10$ for spin systems.[9] This is because in Ref. 9, I used the infinite system method during the second step.

The ultimate success of the TSDMRG depends on the density of the low-lying states in the 1D model. For fixed ms_2 and L, it is, for instance, easier to reach larger $\Delta\epsilon/J_\perp$ in the anisotropic spin one-half Heisenberg model, studied in Ref. 8, than $\Delta\epsilon/t_\perp$ for the tight-binding model as shown in Fig. 2. For $L=16$, $ms_2=96$, and $J_\perp = t_\perp = 0.15$, I find that $\Delta\epsilon/J_\perp \approx 10$, while $\Delta\epsilon/t_\perp \approx 5$. Hence, the TSDMRG method will be more accurate for a spin model than for the tight-binding model. Using the infinite system method during the second step on the anisotropic Heisenberg model with $J_\perp = 0.1$, I can now reach an agreement of about 10^{-6} with the stochastic QMC method.

Two possible sources of error can reduce accuracy in the TSDMRG with respect to the conventional DMRG. They are the truncation of the superblock from $4 \times ms_1$ states to only ms_2 states and the use of three blocks instead of four during the second step. In Table II, I analyze the impact of the reduction of the number of states to ms_2 for three-leg ladders. The choice of three-leg ladders is motivated by the fact that

TABLE II. Ground-state energies of three-leg ladders.

ms_2	8×3	16×3	24×3
64	−0.241524	−0.211929	0.204040
Exact	−0.241524	−0.211931	0.204049

TABLE III. Ground-state energies for different lattice sizes; a single state was targeted in the second step.

ms_2	8×9	16×17	24×25
64	−0.24761	−0.21401	0.20504
100	−0.24819	−0.21414	0.20509
120	−0.24832	−0.21419	
Exact	−0.24857	−0.21432	0.20519

at this point, the TSDMRG is equivalent to the exact diagonalization of three reduced superblocks. It can be seen that as far as $t_\perp \gtrsim \epsilon_0(N_x+1)-\epsilon_0(N_x)$ and $t_\perp \gtrsim \epsilon_0(N_x)-\epsilon_0(N_x-1)$, the TSDMRG at this point is as accurate as the 1D DMRG. Note that the accuracy remains nearly the same irrespective of L as far as the ratio $\Delta\epsilon/t_\perp$ remains nearly constant. Since $\Delta\epsilon$ decreases when L increases, $t_\perp$ must be decreased in order to keep the same level of accuracy for fixed ms_2. In principle, following this prescription, much larger systems may be studied. $\Delta\epsilon/t_\perp$ does not have to be very large, in this case it is about 5, to obtain very good agreement with the exact result.

The second source of error is related to the fact that the effective single site during the second step is now a chain having ms_2 states. I am thus forced to use three blocks instead of four to reduce the computational burden. In Table III, it can be seen that this results in a reduction in accuracy of about 2 orders of magnitude with respect to those of three-leg ladders. These results are nevertheless very good given the relatively modest computer power involved. All calculations were done on a workstation.

The DMRG is less accurate when three blocks are used instead of four. This can be understood by applying the following view on the formation of the reduced density matrix. The construction of the reduced density matrix may be regarded as a linear mapping $u_\Psi: \mathbf{F}^* \rightarrow \mathbf{E}$, where $\mathbf{E}$ is the system, $\mathbf{F}$ is the environment and, $\mathbf{F}^*$ is the dual space of $\mathbf{F}$. Using the decomposition of the superblock wave function $\Psi_{[0]}=\Sigma_i \phi_i^L \otimes \phi_i^R$, with $\phi_i^L \in \mathbf{E}$ and $\Phi_i^R \in \mathbf{F}$, for any $\phi^* \in F^*$,

$$u_\Psi(\phi^*) = \sum_{i=1} \langle \phi^* | \phi_i^R \rangle \phi_i^L. \tag{11}$$

Let $|k\rangle, k=1,\ldots \dim \mathbf{E}$ and $|l\rangle, l=1,\ldots \dim \mathbf{F}$ be the basis of $\mathbf{E}$ and $\mathbf{F}$, respectively. Then, $|l\rangle$ has a dual basis $\langle l^*|$ such that $\langle l^*|l\rangle=\delta_{l,l^*}$. The matrix elements of u_Ψ in this basis are just the coordinates of the superblock wave function $\Phi_{[0]_{k,l}}$. The rank r of this mapping, which is also the rank of the reduced density matrix is always smaller or equal to the smallest dimension of $\mathbf{E}$ or $\mathbf{F}$, $r<\mathrm{Min}(\dim \mathbf{E}, \dim \mathbf{F})$. Hence, if ms_2 states are kept in the two external blocks, the number of nonzero eigenvalues of ρ cannot be larger than ms_2. Consequently, some states which have nonzero eigenvalues in the normal four block configuration will be missing. A possible solution to this problem is to target additional low-lying states above $\Psi_{[0]}(N)$. The weight of these states in ρ must be small so that their role is simply to add the missing states not to be described accurately themselves. A larger weight on these additional states would lead to the reduction of the accuracy for a fixed ms_2. In Table IV, I show the improved energies when, besides the ground state, I target the lowest states of the spin sectors $S_z=-1$ and $S_z=+1$ with N electrons. The weights were, respectively, 0.995, 0.0025, and 0.0025 for the three states. This lowers $E_{[0]}(N)$ in all cases, but the gain does not appear to be spectacular. However, I do not know whether this is due to my choice of perturbation of ρ or whether even the algorithm with four blocks would not yield better $E_{[0]}(N)$. If the lowest sectors with $N+1$ and $N-1$ electrons which have $S_z=\pm 0.5$ are projected instead, I find that the results are similar to those with $S_z=\pm 1$ sectors. There may be many ways to add the missing states. A more systematic approach to this problem has recently been suggested.[15] It is based on using a local perturbation to build a correction to the density matrix from the site at the edge of the system. Here, such a perturbation would be $\Delta\rho=\alpha c_l^\dagger \rho c_l$, where α is a constant $\alpha \approx 10^{-3}-10^{-2}$ and $c_l^\dagger, c_l$ are the creation and annihilation operators of the chain at the edge of the system. This type of perturbation resulted in an accuracy gain of more than an order of magnitude in the case of a spin chain.[15] The three block method was found to be on par with the four block method. It will be interesting to see in a future study how this type of local perturbation performs within the TSDMRG.

TABLE IV. Ground-state energies for different lattice sizes; three states were targeted in the second step: the ground state itself and the lowest states of $S_z=0$ and $S_z=1$ sectors.

ms_2	8×9	16×17
64	−0.24803	−0.21401
100	−0.24828	−0.21417
Exact	−0.24857	−0.21432

To conclude this section, as a first step to the investigation of interacting electron models, I have shown that the TSDMRG can successfully be applied to the tight-binding model. The agreement with the exact result is very good and can be improved since the computational power involved in this study was modest. The extension to the AHM with $U\neq 0$ is straightforward. There is no additional change in the algorithm since the term involving U is local and thus treated during the 1D part of the TSDMRG. The role of U is to reduce $\Delta\epsilon$ as shown in Fig. 3. For fixed L and ms_2, $\Delta\epsilon$ decreases linearly with increasing U. For $L=16$ and $ms_2=128$, I anticipate that for $U\lesssim 3$, the interacting system results will be on the same level or better than those of the noninteracting case with $ms_2=100$ for the same value of L. This is confirmed by a numerical test on a 16×3 system for $U=4$, $V=0.85$, $\mu=0$, and $t_\perp=0.2$, keeping $ms_2=160$. For these parameters $\Delta\epsilon=0.78$, we are at the limit of accuracy of the TSDMRG. The TSDMRG ground-state energy −0.6207 is nevertheless in good agreement with that of the conventional multichain approach −0.6228 with $m=500$.

V. GROUND-STATE PROPERTIES OF COUPLED HUBBARD CHAINS

I now proceed to the study of $U\neq 0$. One of the main motivations for such a study is the possibility to gain insight

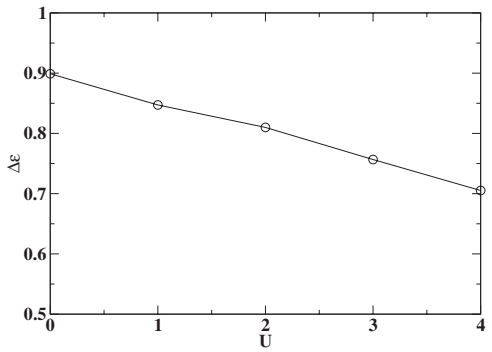

FIG. 3. Width $\Delta\epsilon$ for the low-lying states of the 1D Hubbard chain as function of U for $L=16$ and $ms_2=128$.

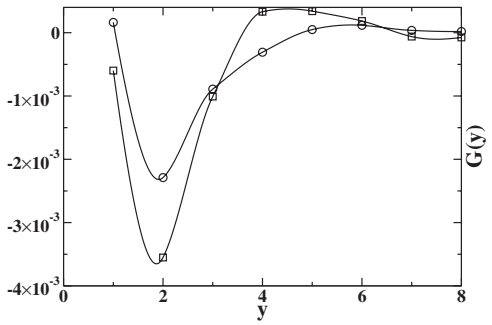

FIG. 4. Transverse Green's function $G(y)$ for $t_d=0$ (circles), $t_d=0.1$ (squares).

into the mechanism of superconductivity in quasi-1D systems. The mechanism of superconductivity in the quasi-1D organic materials Bechgaard and Fabre salts, is still an open issue.[16] Since these materials are 1D above a crossover temperature $T_x \approx t_\perp/\pi$, it is broadly accepted that the starting point for the understanding of their low T behavior should be pure 1D physics. The occurrence of the low T ordered phases is driven by the interchain hopping $t_\perp$. Two main hypotheses have been suggested concerning superconductivity. The first hypothesis (see a recent review in Ref. 16) relies on a more conventional physics: $t_\perp$ drives the system to a 2D electron gas which is an anisotropic Fermi liquid which becomes superconductive through a conventional BCS mechanism. However, it has been argued[17] that given the smallness of $t_\perp$, the resulting electron-phonon coupling would not be enough to account for the observed T_c. The second hypothesis, which has gained strength over the years given the absence of a clear phonon signature, is that the pairing mechanism originates from an exchange of spin fluctuation.[17]

Interest in this issue was recently revived by the NMR Knight-shift experimental finding that the symmetry of the Cooper pairs is triplet[4] in $(TMTSF)_2(PF)_6$. No shift was found in the magnetic susceptibility at the transition for measurement made under a magnetic field of about 1.4 T. A triplet pairing scenario was subsequently supported by the persistence of superconductivity under fields far exceeding the Pauli breaking-pair limit.[18] However, there is no simple explanation of this scenario. Triplet pairing would be unfavorable in a BCS-like scenario for which a singlet s wave is most likely. Triplet pairing is also less likely in the spin-fluctuation mechanism for which a singlet d wave is predicted by analytical RG (Ref. 16) or by perturbative approaches.[19] It has been argued that these difficulties in both mechanisms can be circumvented. In the BCS case, the association of AFM fluctuations with an open Fermi surface to the electron-phonon mechanism may lead to a triplet pairing.[20] In the spin-fluctuation case, the addition of interchain Coulomb interactions may favor a triplet f wave in lieu of the singlet d wave.[16,19,21] The more exotic Fulde-Ferrel-Larkin-Ovchinnikov phase can also be invoked to account for the large paramagnetic limit. However, the Knight-shift result which was thought to bring a conclusion to this long-standing issue has only revived the old controversy. The conclusion of this experiment itself has been recently challenged. In Ref. 22, it was pointed out that the observation of triplet superconductivity claimed in Ref. 4 could be a spurious effect due to the lack of thermalization of the samples. A recent Knight-shift experiment performed at lower fields reveals a decrease in the spin susceptibility. This is consistent with singlet pairing.[5]

The 1D interacting electron gas is now fairly well understood.[6] There is no phase with long-range order. There are essentially four regions in the phase diagram, characterized by the dominant correlations, i.e., spin-density wave (SDW), charge-density wave (CDW), singlet superconductivity (SS), and triplet superconductivity (TS). The essential question is whether the interchain hopping will simply freeze the dominant 1D fluctuation into long-range order (LRO) or create new 2D physics. The estimated values of U and V for the Bechgaard salts suggest that they are in the SDW region in their 1D regime. This suggests that superconductivity in these materials is a 2D phenomenon. Interchain pair tunneling was suggested soon after the discovery of superconductivity in an organic compound.[1] Emery[13] argued that a mechanism similar to the Kohn-Luttinger mechanism might be responsible for superconductivity in the organic materials. When $t_\perp$ is turned on, pairing can arise from exchange of short-range SDW fluctuations. The reason is that the oscillating SDW susceptibility at $Q=(2k_F,k_\perp)$ would have an attractive region if $k_\perp \neq 0$. In particular if $k_\perp=\pi$ as I found, then the interaction would be attractive between particles in neighboring chains. In this study, I will restrain myself to the study of interchain pair tunneling. I was unable to compute correlation functions of pairs in which each electron belongs to a different chain. The reason is that in the DMRG method, for the correlation functions to be accurate, at least two different blocks should be involved. This means that for pair correlation for which each electron of the pair is on a different chain, at least four blocks are needed. However, the introduction of four blocks in the second step of the TSDMRG leads to a prohibitive CPU time.

With the hope of frustrating an SDW ordering which is usually expected, I will add an extra terms to model (1). These are the diagonal interchain hopping

$$H_d = -t_d \sum_{i,l,\sigma} \{(c^\dagger_{i,l,\sigma} c_{i+1,l+1,\sigma} + \text{H.c.}) + (c^\dagger_{i+1,l,\sigma} c_{i,l-1,\sigma} + \text{H.c.})\}, \tag{12}$$

and the next-nearest-neighbor interchain hopping

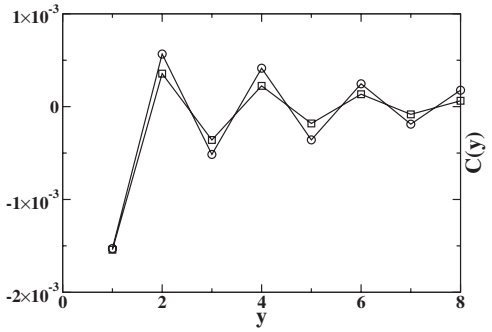

FIG. 5. Transverse spin-spin correlation $C(y)$ for $t_d=0$ (circles), $t_d=0.1$ (squares).

$$H'_{\perp} = -t'_{\perp} \sum_{i,l,\sigma} (c^{\dagger}_{i,l,\sigma} c_{i,l+2,\sigma} + \text{H.c.}).$$

I will also add the interchain Coulomb interaction

$$H_V = V_{\perp} \sum_{i,l} n_{i,l} \, . \, n_{i,l+1} \tag{13}$$

I set $t_{\perp}=0.2$, $ms_1=256$, $ms_2=128$, and $L\times(L+1)=16\times17$. A second set of calculations with $t_{\perp}=0.15$, the same values of ms_1 and ms_2, and $L\times(L+1)=24\times25$ lead to the same conclusions. Therefore, they will not be shown here. In order to analyze the physics induced by the transverse couplings, I compute the following interchain correlations: the transverse single-particle Green's function, shown in Fig. 4,

$$G(y) = \langle c_{L/2,L/2+y} c^{\dagger}_{L/2,L/2+1} \rangle, \tag{14}$$

the transverse spin-spin correlation function, shown in Fig. 5,

$$C(y) = \frac{1}{3} \langle \mathbf{S}_{L/2,L/2+y} \mathbf{S}_{L/2,L/2+1} \rangle, \tag{15}$$

the transverse local pairs singlet superconductive correlation, shown in Fig. 6,

$$SS(y) = \langle \Sigma_{L/2,L/2+y} \Sigma^{\dagger}_{L/2,L/2+1} \rangle, \tag{16}$$

where

$$\Sigma_{i,l} = c_{i,l\uparrow} c_{i,l\downarrow}, \tag{17}$$

the transverse triplet superconductive correlation, shown in Fig. 7,

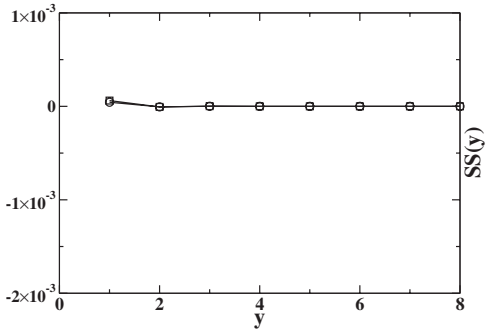

FIG. 6. Transverse local singlet correlation $SS(y)$ for $t_d=0$ (circles), $t_d=0.1$ (squares).

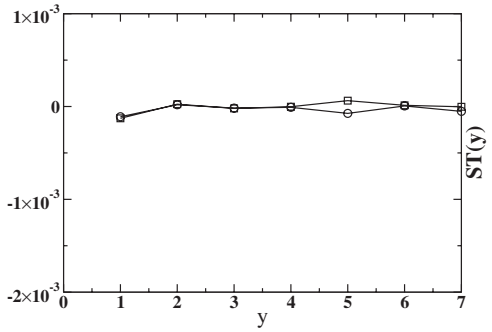

FIG. 7. Transverse triplet superconductive correlation $ST(y)$ for $t_d=0$ (circles), $t_d=0.1$ (squares).

$$ST(y) = 2\langle \Theta_{L/2,L/2+y} \Theta^{\dagger}_{L/2,L/2+1} \rangle, \tag{18}$$

where

$$\Theta_{i,l} = \frac{1}{\sqrt{2}} (c_{i,l\uparrow} c_{i+1,l\downarrow} + c_{i,l\downarrow} c_{i+1,l\uparrow}), \tag{19}$$

and the transverse nonlocal singlet pair superconductive correlation function, shown in Fig. 8,

$$SD(y) = 2\langle \Delta_{L/2,L/2+y} \Delta^{\dagger}_{L/2,L/2+1} \rangle, \tag{20}$$

where

$$\Delta_{i,l} = \frac{1}{\sqrt{2}} (c_{i,l\uparrow} c_{i+1,l\downarrow} - c_{i,l\downarrow} c_{i+1,l\uparrow}). \tag{21}$$

A. Strong-coupling regime

Let us first consider, the regime $U \gtrsim 4$. I choose for instance $U=4$, $V=0.85$, $\mu=0$, and $t_d=t'_{\perp}=V_{\perp}=0$; besides single-particle hopping, $t_{\perp}$ also generates two-particle hopping both in the particle-hole and particle-particle channels. These two-particle correlation functions are roughly given by the average values $t^2_{\perp} \langle c^{\dagger}_{i,l\sigma} c_{i,l-\sigma} c^{\dagger}_{i,l+j-\sigma} c_{i,l+j\sigma} \rangle$ and $t^2_{\perp} \langle c^{\dagger}_{i,l\sigma} c^{\dagger}_{i,l-\sigma} c_{i,l+j\sigma} c_{i,l+j-\sigma} \rangle$ for an on-site pair created at (i,l) and then destroyed at $(i,l+j)$. It is expected that the dominant two-particle correlations are SDW with $k_{\perp}=\pi$. This is seen in Figs. 5–8. The transverse pairing correlations are all found to be small with respect to $C(y)$. Among the pairing correlations, $SS(y)$ decays faster then $ST(y)$ and $SD(y)$.

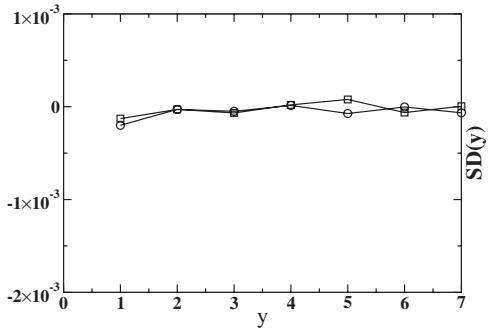

FIG. 8. Transverse singlet nonlocal superconductive correlation $SD(y)$ for $t_d=0$ (circles), $t_d=0.1$ (squares).

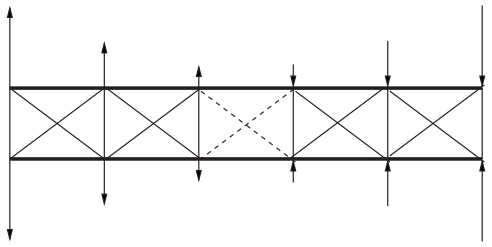

FIG. 9. Sketch of the spin texture (arrows) in two consecutive chains in an SDW. The bold horizontal lines represent the chains. The full diagonal lines show bonds for which t_d tends to increase the SDW order. The diagonal dotted lines show bonds for which t_d frustrates the magnetic order.

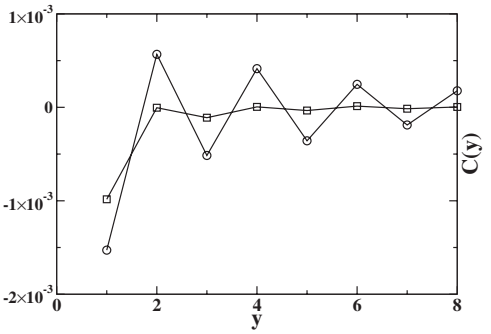

FIG. 10. Transverse spin-spin correlation $C(y)$ for $U=4$ (circles), $U=2$ and $V_\perp=0.4$ (squares).

These results are consistent with the view that the role of $t_\perp$ is to freeze the dominant 1D correlations into LRO.

When $t_d \neq 0$, it is expected that for a strong enough t_d, the magnetic order will vanish because of the frustration induced by t_d. A simple argument is that t_d induces an AFM exchange between next-nearest neighbors on chains l and $l+1$ which compete with the AFM exchange between nearest neighbors. The hope is that there could be a region of the phase diagram where superconductivity could ultimately win either by pair tunneling between the chains or by the Emery's mechanism. However, in Figs. 5–8 it can be seen that, while t_d slightly reduces $C(y)$, the dominant correlations are still SDW even for a strong $t_d/t_\perp=0.5$. $SS(y)$, $ST(y)$, and $SD(y)$ are barely affected by t_d. The fact that t_d does not strongly affect the SDW order can be understood in the light of recent study of coupled $t-J$ chains.[9] It was shown that the frustration strongly suppresses magnetic LRO only close to half filling. For large dopings, two neighboring spins in a chain do not always point to opposite directions as the consequence and t_d does not necessarily frustrate the magnetic order. This is illustrated in a simple sketch in Fig. 9. t_d could even enhance it as seen in the study of $t-J$ chains. In Fig. 4, it can be seen that t_d enhances $G(y)$. This enhancement, together with the decrease of $C(y)$, suggests a possible widening of an eventual Fermi-liquid region at finite T above the ordered phase. When $t_\perp \neq 0$, I also found (not shown) that magnetic correlations are not effectively suppressed even when $t'_\perp=t_\perp/2$. For this value, it would be expected that the ratio of the effective exchange term generated by $t'_\perp$ to that generated by $t_\perp$ is about one quarter. In the frustrated J_1-J_2 spin chain, a spin gap opens around this ratio. This simple picture does not seem to work here.

B. Weak-coupling regime

I now turn in to the regime where $U \lesssim 4$. I set $U=2$, $V=0$, $\mu=-0.9271$, $t_\perp=0.2$, $t_d=0$, and $V_\perp=0.4$, where $V_\perp$ is the interchain Coulomb interaction between nearest neighbors. It can be seen in Fig. 10 that $C(y)$ is now strongly reduced with respect to its strong-coupling values. It is already within our range numerical error for the next-nearest neighbor in the transverse direction. This is an indication that the ground state is probably not an SDW. It is to be noted that this occurs even in the absence of t_d or $t'_\perp$. This seems to be at variance with the RG analysis which requires $t'_\perp$ to destroy the magnetic order.[21] A possible explanation of this is that at half filling, the perfect nesting occurs at the wave vector $Q=(\pi,\pi)$ for the spectrum of Eq. (10). Away from half filling, the nesting is no longer perfect, which leads to the reduction of magnetic correlations. The first correction to the nesting is an effective frustration term which is roughly $t_\perp^2 \cos 2k_\perp$. This expression is identical to a term that could be generated by an explicit frustration $t'_\perp=t_\perp^2$. The discrepancy between the TSDMRG and the RG results could be that this nesting deviation is underevaluated in the RG analysis. This mechanism cannot be invoked in the strong-coupling regime where band effects are small.

The suppression of magnetism is concomitant to a strong enhancement of the singlet-pairing correlations as seen in Fig. 12. Triplet correlations, shown in Fig. 11, remain very small. However, it is clear from the behavior of $C(y)$ that the ground state is nonmagnetic. This result strongly suggests that the ground state is a superconductor in this regime. A finite-size analysis is, however, necessary to conclude whether this persists to the thermodynamic limit. I cannot rule out the possibility of a Fermi-liquid ground state, which is implied by strong single-particle correlations.

VI. APPLICATION TO THE PHYSICS OF ORGANIC CONDUCTORS

The pressure variation will be mimicked by varying the Coulomb parameters U and V, while I keep $t_\parallel$, $t_\perp$, and $V_\perp$ constant in most simulations. In the regime of strong U and

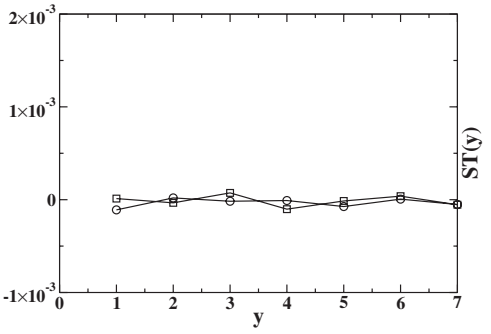

FIG. 11. Transverse triplet superconductive correlation $ST(y)$ for $U=4$ (circles), $U=2$ and $V_\perp=0.4$ (squares).

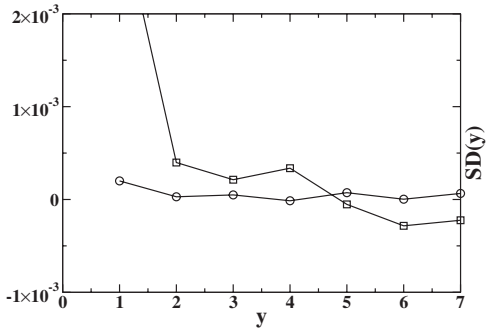

FIG. 12. Transverse singlet nonlocal superconductive correlation $SD(y)$ for $U=4$ (circles), $U=2$ and $V_\perp=0.4$ (squares).

V, the isolated chains are Mott insulators, there is a large charge gap Δ_ρ while the spin degrees of freedom are gapless. At $V \lesssim 2$ for any value of U, there is an insulator-metal transition.[23] The transverse correlation functions yield information on which type of order will dominate. Since the parallel correlations have a power-law decay in absence of a gap, the most dominant transverse correlation in a given channel will automatically lead to long-range order in that channel, even if it is not dominant in 1D. Before performing the analysis of the transverse correlations, it is somewhat instructive to look at the low energy spectrum provided by the Wilson method. This will allow us to make a qualitative comparison with the evolution under pressure with the prediction of the perturbative RG.

The low energy-excitation spectrum of $\tilde{H}$ was obtained from the Wilson RG for $\Lambda \approx 1.2$ for a lattice size 16×6, keeping 100 states block. The lowest 1000 excited states are shown in Fig. 13. They are drastically different as pressure is varied. In the confined regime for $U=6$ $V=2$ Fig. 13(a), all the lowest states have the charge $\lambda_n=0$. This is consistent with the fact that since $t_\perp \ll \Delta_\rho$, the low energy behavior of $\tilde{H}$ is roughly identical to that of Heisenberg model, only spin excitations are allowed. This is typically the regime of Fabre salts at ambient pressure where a large charge gap is observed in optical conductivity measurements.[24] By contrast, in the SDW regime for $U=4$ $V=0.85$, spins excitation are still the lowest but excitations with $\lambda = \pm 1$ now appear above them. Excitations with $\lambda = \pm 2$ are also observed at higher energy. In the regime with important superconductive correlations $U=2$ $V=0$, excitations with $\lambda = \pm 2$ now appear closer to the ground state. This suggests that an appropriate choice of the transverse perturbations could favor interchain two-particle tunneling.

I now analyze the evolution of the transverse correlations when U and V are varied using the two-step DMRG for the lattice size $L_x \times L_y = 16 \times 17$. I keep $ms_1=256$ states during the first step and a maximum of $ms_2=128$ states during the second step. For this value of ms_2, $\Delta E/t_\perp \approx 5$ which means that we are at the limit of the two-step method. Starting from the left of the AFM phase where U and V are expected to be strong, because of the presence of a large Δ_ρ, the carriers are confined in the chains, even when $t_\perp \ll \Delta_\rho$ is turned on. The carrier confinement was observed by Vescoli *et al.*[25] in optical reflectivity measurements. When the oscillating electric

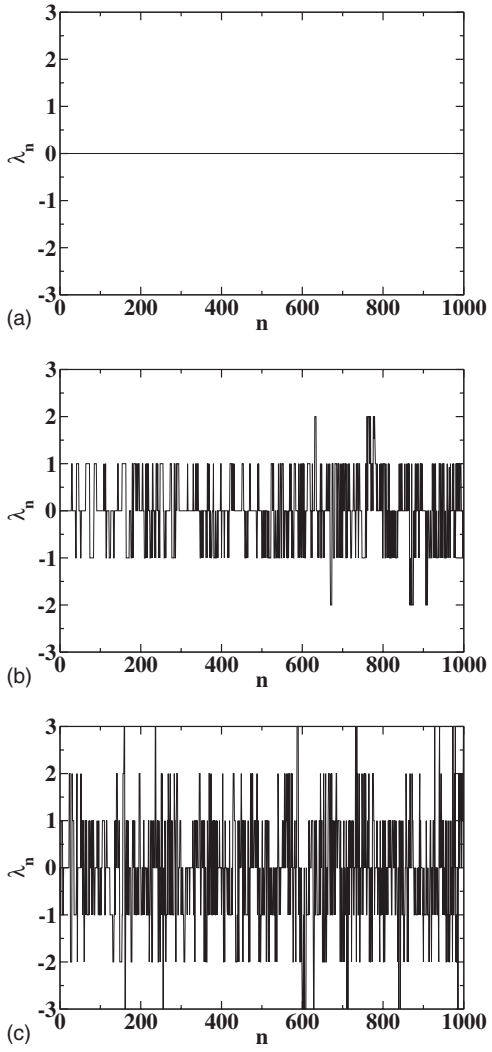

FIG. 13. Charge λ_n of lowest 1000 excitations after six RG iterations, the lattice size is 16×6, for $\Lambda=1.2$: (a) in the localized AFM $U=6$, $V=2$, (b) the SDW $U=4$, $V=0.85$, (c) and superconductor $U=2$, $V=0$. $t_\perp=0.2$ and $V_\perp=0.4$ in all cases.

field was oriented in the transverse direction, no plasma mode was observed. This carrier confinement is seen in the behavior of the transverse Green's function $G(y) = \langle c_{L/2,L/2+y} c^\dagger_{L/2,L/2+1} \rangle$. $G(y)$, shown in Fig. 14(a) for $U=6$ and $V=2$, decays very fast. $G(y) \approx 0$ for $y > 3$. This was expected given that $t_\perp/\Delta_\rho \approx 0.1$. However, as predicted by the RG,[6] although irrelevant, $t_\perp$ can nevertheless generate the motion of transverse spin degrees of freedom and lead to magnetic order. This is seen the transverse spin-spin correlation function $C(y) = \frac{1}{3} \langle \mathbf{S}_{L/2,L/2+y} \mathbf{S}_{L/2,L/2+1} \rangle$ which is shown in Fig. 14(b). I find that despite the irrelevance of $t_\perp$, $G(y)$ has its largest amplitude in the strong-coupling limit. As expected, I find that the transverse singlet (triplet) superconductive correlations $SS(y) = 2\langle \Delta_{L/2,L/2+y} \Delta^\dagger_{L/2,L/2+1} \rangle$ $(ST(y) = 2\langle \Theta_{L/2,L/2+y} \Theta^\dagger_{L/2,L/2+1} \rangle)$, where $\Delta_{i,l} = \frac{1}{\sqrt{2}}(c_{i,l\uparrow} c_{i+1,l\downarrow} - c_{i,l\downarrow} c_{i+1,l\uparrow})$ $(\Theta_{i,l} = \frac{1}{\sqrt{2}}(c_{i,l\uparrow} c_{i+1,l\downarrow} + c_{i,l\downarrow} c_{i+1,l\uparrow}))$ are negligible in this limit as seen in Figs. 14(c) and 14(d).

Moving toward the right of the phase diagram by increasing pressure or equivalently decreasing U and V, the carriers

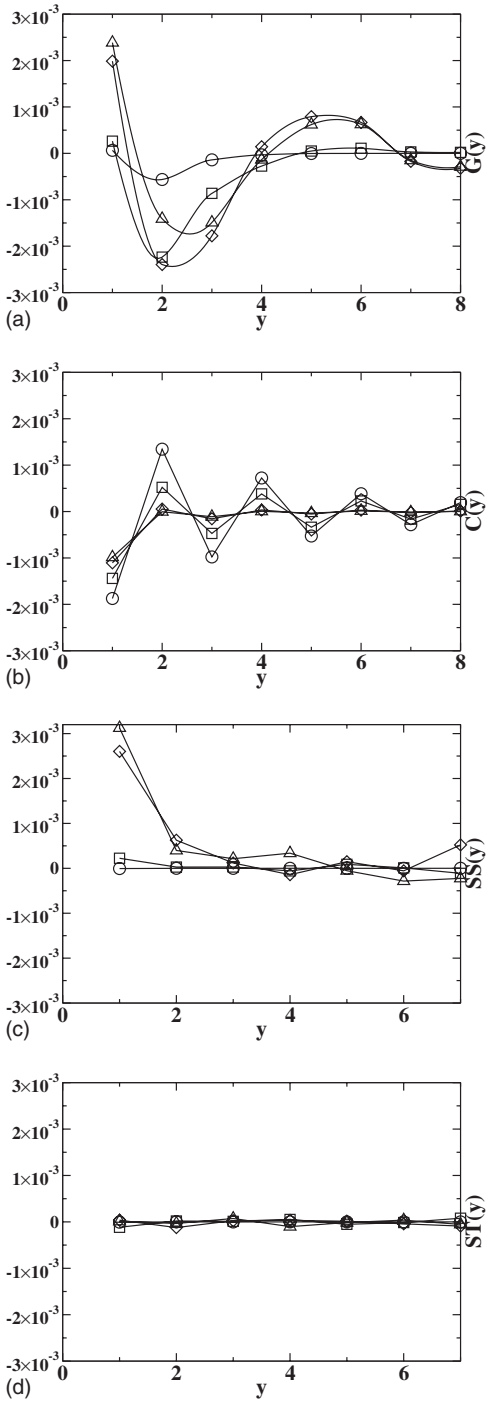

FIG. 14. Transverse interchain correlations as function of distance y: (a) Green's function $G(y)$, (b) spin-spin correlation $C(y)$, (c) singlet superconductive $SS(y)$, (d) triplet superconductive $ST(y)$ for $U=6$, $V=2$ (circles), $U=4$, $V=0.85$ (squares), $U=3$, $V=0$ (diamonds), $U=2$, $V=0$ (triangles). $t_\perp=0.2$ and $V_\perp=0.4$ in all cases.

are expected to progressively deconfine. In this regime, the reflectivity measurements of Ref. 25 reported the observation of a transverse plasma mode. The carrier deconfinement is expected for $t_\perp/\Delta_\rho \approx 0.5$. For $U=4$ and $V=0.85$, the numerical simulation yields $t_\perp/\Delta_\rho \approx 0.3$. In Figs. 14(a)–14(d), it can be seen that for $U=4$ and $V=0.85$ $G(y)$ now has a nonzero amplitude; $C(y)$ is still significant, while $SS(y)$ and $ST(y)$ are still very small. This suggests that the system is in the SDW phase. The perturbative RG, coming from high temperatures, shows that there is a 1D to 2D crossover at $T_x \approx t_\perp/\pi$. At T_x the 1D RG equations cease to be valid. FL arguments are used to describe the onset of the SDW order. The experimental observations are however that both the non-FL and FL characters seem to be present depending on the quantity measured.[6]

If U and V are further reduced, $C(y)$ now decays faster despite the fact that the amplitude of $G(y)$ is larger. $C(y)$ now vanishes for $y>3$ as seen in Fig. 14(b) for $U=3$, $U=2$ and $V=0$ in both cases. This implies the absence of long-range magnetic order in this regime. At the same time, $SS(y)$ sharply increases, suggesting the onset of superconductivity in agreement with the phase diagram. The values of $SS(y)$ at long distances are however within our margin of error. The presence of $V_\perp$ is crucial to the suppression of magnetism and to the enhancement of pairing correlation. In the absence of $V_\perp$, if all other parameters are unchanged, the dominant correlations are AFM. $V_\perp$ induces charge modulation in the transverse direction. Two nearest-neighbor electrons on a given chain take advantage of this modulation to jump on the closest chain. This is reminiscent of the non-BCS scenario suggested by Kohn and Luttinger.[10] In this process, singlet pairs are favored, as seen by the fact that $ST(y)$ is still negligible.

Experimental results on the symmetry of the pairs are still controversial. Knight-shift experiments from different groups have predicted singlet[5] and triplet[4] pairings as discussed in the introduction. This study shows a tendency toward singlet pairing only in the extended Hubbard model. Singlet pairing, though interchain, was also predicted by the perturbative RG. However, in the RG, the pairs could be formed by carriers lying on neighboring chains and AFM was suppressed by hopping to next-nearest-neighbor chain. It was suggested in the RG study that the pairing could be triplet in presence of strong enough next-nearest-neighbor hopping and nearest-neighbor Coulomb interaction both in the transverse direction. The two-step results do not however settle this issue. Many small effects including longer range hopping and Coulomb interactions or the electron-phonon interaction were not included in this simple model. Triplet superconductivity could emerge from these terms. The two-step method provides an efficient method to analyze these different perturbations.

VII. CONCLUSION

In this paper, I presented a TSDMRG study of the competition between magnetism and superconductivity in an anisotropic Hubbard model. I analyzed the effect of the interchain hoppings, $t_\perp, t_d, t'_\perp$, and of the interchain Coulomb interaction $V_\perp$ in the strong and weak U regimes. In the strong-coupling regime, the results are consistent with earlier predictions that the role of $t_\perp$ is to freeze the dominant 1D SDW correlations into a 2D ordered state. However, this is only true in the strong U regime. In this regime, I find that even the introduction of frustration does not disrupt the SDW

order which remains robust up to large values of the frustration. In the weak-coupling regime, singlet pair correlations are dominant. The ground state seems to be a superconductor. This behavior is in agreement with experiments in the Bechgaard or Fabre salts: (i) localized magnetism in the strong-coupling regime, (ii) delocalized SDW magnetism in the intermediate coupling regime, and (iii) superconductivity of singlet type in the weak-coupling regime. Pair hopping is favored by the density fluctuations due to $V_\perp$ as in the KL mechanism.

I have not discussed the spin-Peierls phase which rests at the extreme left of the phase diagram. In this regime, the electron-phonon coupling is dominant over the effective transverse exchange $J_\perp$, hence a pure 1D study of a spin model coupled to phonons such as that of Ref. 26, which shows a spin gap opening, captures this part of the phase diagram.

In this work, heuristic considerations inspired by the experimental phase diagram led me to be concerned only with the search for a regime of parameters where (i) SDW correlations are dominant in the 1D regime and (ii) superconductivity is dominant over magnetism when transverse motion sets in. I did not analyze CDW correlations. These are likely to be important, given that I applied open boundary conditions which are known to generate Friedel oscillations[27] that decay slowly from the boundaries. The CDW correlations are also enhanced by $V_\perp$. Hence, I cannot rule out the possibility of a CDW ground state instead of a superconductor, or even a coexistence of the two ground states, in the regime were pairing is enhanced. However, this work clearly shows that if there is superconductivity in the extended Hubbard model, it is generated by interchain Coulomb interactions.

ACKNOWLEDGMENTS

I am most grateful to C. Bourbonnais for very helpful exchanges. I wish to thank A. M.-S. Tremblay for helpful discussions. I thank E. Jeckelmann for the DMRG data. I also thank V. Lieberman for reading the manuscript. This work was supported by NSF Grant No. DMR-0426775.

[1] D. Jerome and H. J. Schulz, Adv. Phys. **31**, 299 (1982).
[2] C. Bourbonnais and D. Jérome, in *Advance in Synthetic Metals*, edited by P. Bernier, S. Lefrant, and G. Bidan (Elsevier, New York, 1999), p. 206.
[3] T. Giamarchi, *Quantum Physics in One Dimension* (Clarendon, Oxford, 2004), p. 254–269.
[4] I. J. Lee, S. E. Brown, W. G. Clark, M. J. Strouse, M. J. Naughton, W. Kang, and P. M. Chaikin, Phys. Rev. Lett. **88**, 017004 (2001).
[5] Y. Shinagawa, Y. Kurosaki, F. Zhang, C. Parker, S. E. Brown, D. Jérome, J. B. Christensen, and K. Bechgaard, Phys. Rev. Lett. **98**, 147002 (2007).
[6] C. Bourbonnais and L. G. Caron, Int. J. Mod. Phys. B **5**, 1033 (1991).
[7] C. Bourbonnais and L. G. Caron, Europhys. Lett. **5**, 209 (1988).
[8] S. Moukouri, Phys. Rev. B **70**, 014403 (2004).
[9] S. Moukouri, J. Stat. Mech.: Theory Exp. (2006) P02002.
[10] W. Kohn and J. M. Luttinger, Phys. Rev. Lett. **15**, 524 (1965).
[11] S. Biermann, A. Georges, A. Lichtenstein, and T. Giamarchi, Phys. Rev. Lett. **87**, 276405 (2001).
[12] S. R. White, D. J. Scalapino, R. L. Sugar, E. Y. Loh, J. E. Gubernatis, and R. T. Scalettar, Phys. Rev. B **40**, 506 (1989).
[13] S. R. White, Phys. Rev. Lett. **69**, 2863 (1992); Phys. Rev. B **48**, 10345 (1993).
[14] K. G. Wilson, Rev. Mod. Phys. **47**, 773 (1975).
[15] S. R. White, Phys. Rev. B **72**, 180403(R) (2005).
[16] N. Dupuis, C. Bourbonnais, and J. C. Nickel, Fiz. Nizk. Temp. **32**, 505 (2006).
[17] V. J. Emery, Synth. Met. **13**, 21 (1986).
[18] I. J. Lee, M. J. Naughton, and P. M. Chaikin, Physica B **294-295**, 413 (2001).
[19] Y. Tanaka and K. Kuroki, Phys. Rev. B **70**, 060502(R) (2004).
[20] M. Kohmoto and M. Sato, Europhys. Lett. **56**, 736 (2001).
[21] J. C. Nickel, R. Duprat, C. Bourbonnais, and N. Dupuis, Phys. Rev. Lett. **95**, 247001 (2005).
[22] D. Jerome, Chem. Rev. (Washington, D.C.) **104**, 5565 (2004); D. Jerome and C. R. Pasquier, in *Superconductors*, edited by A. V. Narlikar, (Springer-Verlag, Berlin, 2005).
[23] F. Mila and X. Zotos, Europhys. Lett. **24**, 133 (1993).
[24] A. Schwartz, M. Dressel, G. Gruner, V. Vescoli, L. Degiorgi, and T. Giamarchi, Phys. Rev. B **58**, 1261 (1998).
[25] V. Vescoli, L. Degiorgi, W. Henderson, G. Gruner, K. P. Starkey, and L. K. Montgomery, Science **281**, 1181 (1998).
[26] L. G. Caron and S. Moukouri, Phys. Rev. Lett. **76**, 4050 (1996).
[27] S. R. White, Ian Affleck, and D. J. Scalapino, Phys. Rev. B **65**, 165122 (2002).